EMBO reports

scientific report

Structural basis for recognition of H3K4 methylation status by the DNA methyltransferase 3A ATRX–DNMT3–DNMT3L domain

Junji Otani[1], Toshiyuki Nankumo[2], Kyohei Arita[1], Susumu Inamoto[3+], Mariko Ariyoshi[1++] & Masahiro Shirakawa[1+++]

[1]Department of Molecular Engineering, Graduate School of Engineering, Kyoto University, Kyoto, Japan, [2]Department of Supramolecular Biology, Yokohama City University, Yokohama, Japan, and [3]Department of Human Genome Research, Kazusa DNA Research Institute, Chiba, Japan

DNMT3 proteins are *de novo* DNA methyltransferases that are responsible for the establishment of DNA methylation patterns in mammalian genomes. Here, we have determined the crystal structures of the ATRX–DNMT3–DNMT3L (ADD) domain of DNMT3A in an unliganded form and in a complex with the amino-terminal tail of histone H3. Combined with the results of biochemical analysis, the complex structure indicates that DNMT3A recognizes the unmethylated state of lysine 4 in histone H3. This finding indicates that the recruitment of DNMT3A onto chromatin, and thereby *de novo* DNA methylation, is mediated by recognition of the histone modification state by its ADD domain. Furthermore, our biochemical and nuclear magnetic resonance data show mutually exclusive binding of the ADD domain of DNMT3A and the chromodomain of heterochromatin protein 1α to the H3 tail. These results indicate that *de novo* DNA methylation by DNMT3A requires the alteration of chromatin structure.

Keywords: DNA methyltransferase; histone modification; heterochromatin protein 1; crystal structure; NMR

EMBO reports (2009) **10,** 1235–1241. doi:10.1038/embor.2009.218

[1]Department of Molecular Engineering, Graduate School of Engineering, Kyoto University, Kyoto-Daigaku Katsura, Nishikyo-Ku, Kyoto 615-8510, Japan
[2]Department of Supramolecular Biology, Yokohama City University, 1-7-29 Suehiro-cho, Tsurumi-ku, Yokohama 230-0045, Japan
[3]Department of Human Genome Research, Kazusa DNA Research Institute, 2-6-7 Kazusa-Kamatari, Kisarazu, Chiba 292-0818, Japan
[+]Corresponding author. Tel: +81 438 52 3506; Fax: +81 438 52 3921; E-mail: inamots@kazusa.or.jp
[++]Corresponding author. Tel: +81 75 383 2536; Fax: +81 75 383 2541; E-mail: ariyoshi@moleng.kyoto-u.ac.jp
[+++]Corresponding author. Tel: +81 75 383 2535; Fax: +81 75 383 2541; E-mail: shirakawa@moleng.kyoto-u.ac.jp

Received 30 March 2009; revised 28 July 2009; accepted 24 August 2009; published online 16 October 2009

INTRODUCTION

DNA methylation is one of the principal epigenetic marks associated with a repressed chromatin state and gene silencing, and it regulates various physiological events such as X-chromosome inactivation, embryogenesis and genomic imprinting (Bird, 2002). In mammals, cytosine methylation at the C5 position in CpG dinucleotides is the only covalent modification of genomic DNA under physiological conditions. The *de novo* establishment of DNA methylation patterns in early mammalian development involves the DNA methyltransferase (DNMT) 3 family members DNMT3A and DNMT3B, and the DNMT3-like non-enzymatic regulatory factor DNMT3L (Goll & Bestor, 2005). DNMT3L has been shown to recognize unmethylated lysine 4 (Lys 4) of histone H3 (H3K4me0) through its alpha thalassaemia/mental retardation syndrome X-linked homologue (ATRX)–DNMT3–DNMT3L (ADD) domain, indicating that the DNMT3A–DNMT3L complex is targeted to chromatin containing H3K4me0 (Ooi *et al*, 2007). Genome-wide analyses have also shown that the chromatin regions tagged with methylated H3K4 are protected from CpG methylation (Okitsu & Hsieh, 2007; Weber *et al*, 2007).

In mammals, *de novo* DNA methylation in pericentric heterochromatin requires trimethylation of Lys 9 in histone H3 (H3K9me3) by H3K9 histone methyltransferases (HMTases), Suv39h1/2, and the subsequent binding of heterochromatin protein 1 (HP1) to H3K9me3 (Lehnertz *et al*, 2003). Conversely, DNA methylation in euchromatic regions has been suggested to involve HMTase G9a, which catalyses monomethylation and dimethylation of H3K9 (El Gazzar *et al*, 2008). Recently, G9a has been shown to interact directly with DNMT3A/B and to facilitate *de novo* DNA methylation in early embryonic gene promoters independently of its HMTase activity (Epsztejn-Litman *et al*, 2008; Tachibana *et al*, 2008). Thus, the mechanism of DNMT3 recruitment for *de novo* methylation might be different for heterochromatin and euchromatin regions, and a complex scheme of interplay between *de novo* DNA methylation and histone modifications has recently emerged. However, little is yet known

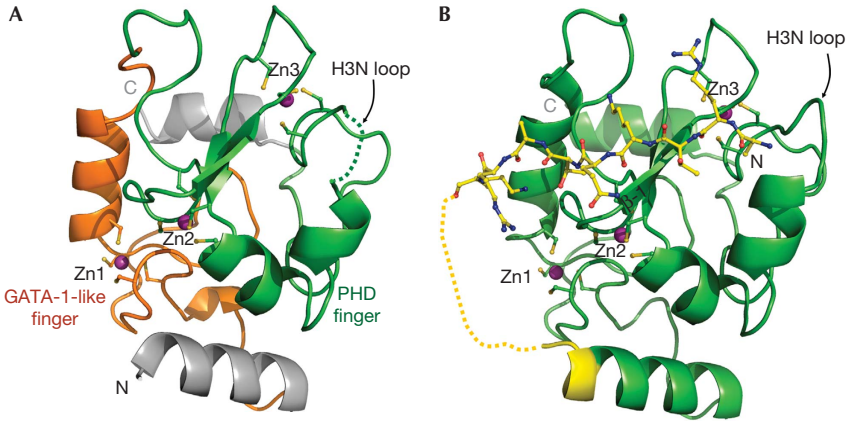

Fig 1 | Overall structures of ADD_{3A} in the unliganded and H3-bound forms. (**A**) Ribbon representation of the ligand-free ADD_{3A}. Three zinc ions and cysteine residues forming CxxC motifs are shown as magenta spheres and multicoloured stick models, respectively. GATA1-like and PHD fingers are shown in orange and green, respectively. The green dotted line represents the disordered H3N loop. (**B**) Crystal structure of ADD_{3A} (green) bound to the H3 tail (yellow). H3 peptide (residues 1–9) is shown as a ball-and-stick model. The disordered linker peptide that connects the carboxy-terminus of the peptide and the amino-terminus of ADD_{3A} is represented by a yellow dotted line. ADD_{3A}, ADD domain of DNMT3A; GATA1, GATA binding protein 1; PHD, plant homeodomain.

about molecular mechanisms regulating the hierarchical order and/or cooperative action of these epigenetic traits.

Here, we report the crystal structures of the ADD domain of DNMT3A (ADD_{3A}) in a ligand-free form and in complex with the peptide derived from the amino-terminal tail of histone H3 (H3 tail), and thereby provide structural insight into recognition of histone H3 by the ADD domain at atomic resolution. Together with biochemical data, the crystal structures have shown that ADD_{3A} binds specifically to H3K4me0. Our finding indicates that the ADD domains of the DNMT3 family have a decisive role in blocking DNMT activity in the areas of the genome with chromatin containing methylated H3K4. In addition, our biochemical and nuclear magnetic resonance (NMR) data have shown that ADD_{3A} competes with the chromodomain (CD) of heterochromatin protein 1α (HP1α; $CD_{HP1\alpha}$) for binding to the H3 tail. Considering the previous observations of the recruitment of DNMTs to chromatin that is mediated by HP1 proteins (Jackson *et al*, 2002; Fuks *et al*, 2003), our results indicate that ADD_{3A} might promote the local chromatin structure conversion required for the catalytic activity of DNMT3A by temporarily displacing HP1α.

RESULTS

Crystal structure of the DNMT3A ADD domain

The crystal structure of the ligand-free ADD_{3A} was determined by using the multiple-wavelength dispersion method with intrinsic zinc atoms at a resolution of 2.3 Å (Fig 1A; supplementary Fig S1A online). The electron densities for four residues in a loop region (residues 577–580) and the carboxy-terminal five residues (residues 610–614) were not observed, indicating structural disorder in these regions. The overall structure of ADD_{3A} is similar to that of the ADD domains of DNMT3L (ADD_{3L}) and ATRX (Argentaro *et al*, 2007; Ooi *et al*, 2007), and is composed of two C_4-type zinc fingers: GATA binding protein 1 (GATA1) and plant homeodomain (PHD)-type (supplementary Fig S1B online). The histone-binding-surface character of DNMT3L seemed well conserved in the structure of ADD_{3A} (supplementary Fig S1C online).

Table 1 | Dissociation constants of the interaction between ADD/CD and H3/H4-tail peptides determined by isothermal titration calorimetry measurements or nuclear magnetic resonance titration experiments

Method	Protein	Peptide	K_D value (μM)
ITC	ADD_{3A}	$H3_{1-19}$	0.26
ITC	ADD_{3A}	$H3_{1-10}$	0.75
ITC	ADD_{3A}	$H3K4me0_{1-19}$*	0.57 ± 0.05‡
ITC	ADD_{3A}	$H3K4me2_{1-19}$*	4.0 ± 0.3‡
ITC	ADD_{3A}	$H3K4me3_{1-19}$*	6.8 ± 0.1‡
ITC	ADD_{3A}	$H3K9me2_{1-19}$*	0.23
ITC	ADD_{3A}	$H3K9me3_{1-19}$*	0.25 ± 0.01‡
ITC	ADD_{3A}	$H3_{1-19}$ K9C	0.50
ITC	ADD_{3A}	$H3R2me2a_{1-15}$	0.74
ITC	ADD_{3A}	Ac-$H3_{1-19}$	Not detected
NMR	ADD_{3A}	Ac-$H3_{1-19}$	128
ITC	ADD_{3A}	Ac-$H4_{1-20}$	Not detected
NMR	ADD_{3A}	Ac-$H4_{1-20}$	150
ITC	ADD_{3A}	Ac-$H4R3me2s_{1-20}$	Not detected
NMR	ADD_{3A}	Ac-$H4R3me2s_{1-20}$	250
ITC	ADD_{3L}	$H3_{1-19}$	3.4 ± 0.87‡
ITC	$CD_{HP1\alpha}$	$H3K9me3_{1-19}$*	1.3 ± 0.05‡
NMR	$CD_{HP1\alpha}$	$H3K9me3_{1-19}$*	3.6 ± 1.3§
NMR	$CD_{HP1\alpha}$	$H3K9me2_{1-19}$*	7.0 ± 3.2§

*Methylated lysine analogue peptide.
‡Means of two experiments (mean ± deviations).
§Values obtained from competitive NMR binding experiment (see supplementary methods online).
Ac, acetylated; $ADD_{3A/3L}$, ADD domain of DNMT3A/3L; $CD_{HP1\alpha}$, chromodomain of HP1α; HP1α, heterochromatin protein 1α; ITC, isothermal titration calorimetry; NMR, nuclear magnetic resonance.

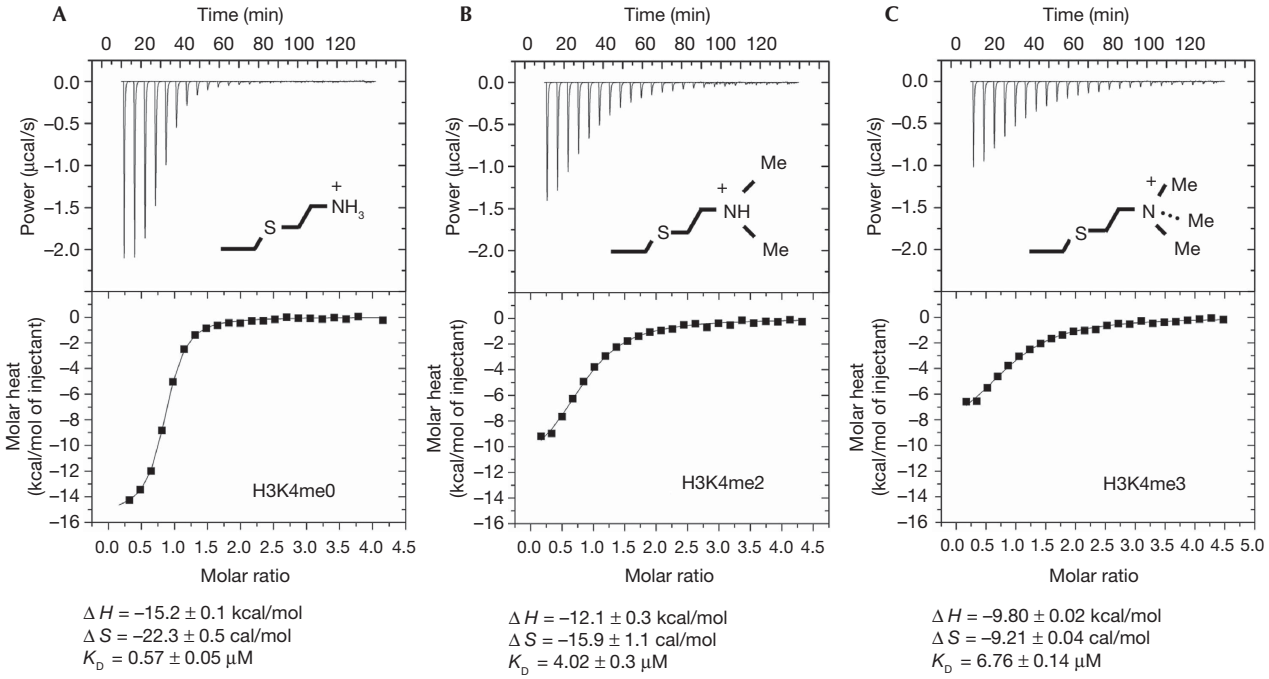

Fig 2 | Calorimetric study of the binding of ADD_{3A} to $H3_{1–19}$ peptides containing non-methylated (**A**), dimethylated (**B**) or trimethylated (**C**) H3K4 analogues. ΔS, ΔH and K_D values are the means of two experiments that used different peptide and protein concentrations. $H3_{1–19}$, amino-terminal 19 amino acids of histone H3.

Histone H3 binding ADD_{3A}

We examined the binding of ADD_{3A} to the H3 tail using isothermal titration calorimetry (ITC). ADD_{3A} binds to peptides with the sequences of the N-terminal 19 and 10 amino acids of histone H3 (designated as $H3_{1–19}$ and $H3_{1–10}$, respectively) with high affinities. The dissociation constant, K_D, is 0.26 μM and 0.75 μM for $H3_{1–19}$ and $H3_{1–10}$, respectively (Table 1). To analyse the effect of the methylation of H3K4 on the interaction between ADD_{3A} and the H3 tail, we introduced analogues of non-methylated, dimethylated and trimethylated lysine at the position of Lys 4 in $H3_{1–19}$ according to a recently developed procedure (Simon *et al*, 2007), and measured their affinities for ADD_{3A} using ITC. The affinity of the $H3_{1–19}$ peptide harbouring an H3K4me0 analogue for ADD_{3A} ($K_D = 0.57 \pm 0.05$ μM) was slightly smaller than that of the native $H3_{1–19}$ (Fig 2A; Table 1). Nevertheless, the analogue peptide seemed to mimic the native peptide effectively (supplementary information online). Conversely, the H3K4me2 and H3K4me3 analogue peptides showed roughly 10-fold lower affinities for ADD_{3A}, with K_D values of 4.02 ± 0.3 μM and 6.76 ± 0.14 μM, respectively (Fig 2B,C and Table 1). Hence, ADD_{3A} specifically recognizes the non-methylated state of H3K4. Weaker binding to the H3 tail containing methylated H3K4 analogue is consistent with previous observations showing protection of H3K4 methylated regions from DNA methylation (Okitsu & Hsieh, 2007; Weber *et al*, 2007).

During the preparation of this paper, a work was published reporting that symmetrical methylation of Arg 3 in histone H4 (H4R3me2s) and its subsequent recognition by ADD_{3A} are required for DNA methylation at the human *β-globin* locus, leading to silencing of the embryo-specific genes (Zhao *et al*, 2009). However, we could not reproduce the interaction between ADD_{3A} and the H4R3me2 s peptide under our experimental conditions (Table 1; supplementary information online).

Recognition of non-methylated H3K4 by ADD_{3A}

We also determined the crystal structure of ADD_{3A} bound to the H3 tail (Fig 1B). In the ligand-free crystal structure, the N-terminus of ADD_{3A} is located in the vicinity of a putative histone-binding groove (Fig 1A). We then linked a peptide consisting of the N-terminal 20 residues of histone H3 to the N-terminus of ADD_{3A} by expressing an H3 peptide–ADD_{3A} fusion protein (supplementary information online), obtained crystals suitable for X-ray diffraction experiments and determined the crystal structure of the linked complex at 2.3 Å resolution. The electron density map allowed us to build a model of the H3 peptide, except for the amino-acid residues from 10 to 16.

As commonly observed in PHD fingers–H3 tail complexes, the extended H3 peptide fits into a shallow groove on the PHD-finger motif in ADD_{3A}, resulting in 721 $Å^2$ of total buried surface area (Fig 3A; supplementary Fig S2 online). The segment from Arg 2 to Thr 6 forms intermolecular main-chain hydrogen bonds with strand β1 of ADD_{3A} (residues 541–545), resulting in a continuous three-stranded antiparallel β-sheet. On binding to the H3 tail, a conformational change is induced in the H3 N-terminus recognition loop (H3N loop; residues 577–580) of ADD_{3A}, which is disordered in the ligand-free form. The H3N loop is fixed by hydrogen bonds between the terminal amino group of the H3 tail and the main-chain carbonyl oxygen atoms of Ala 575, Ile 576 and

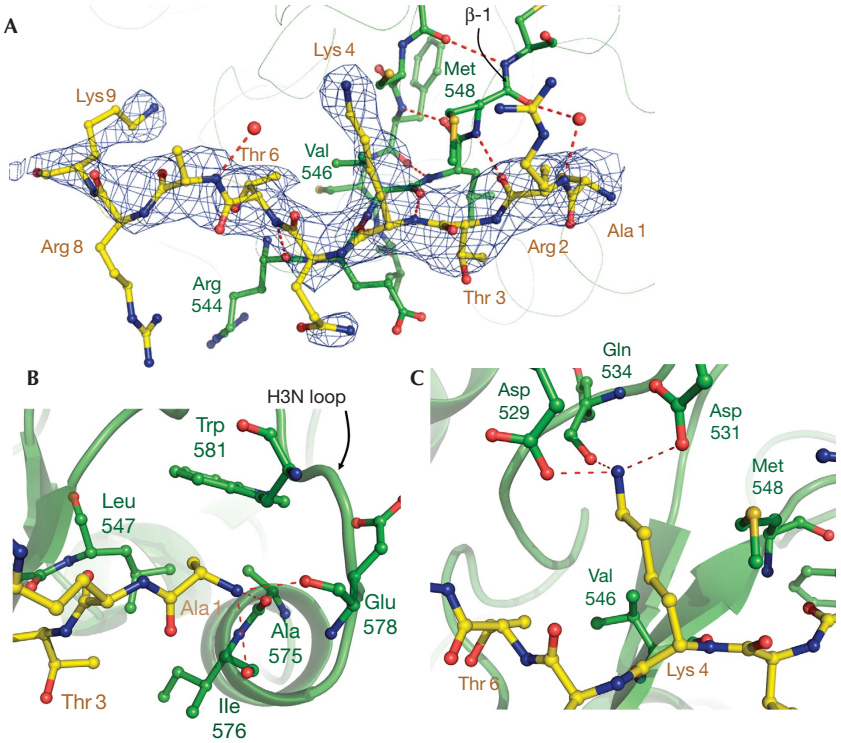

Fig 3 | Recognition of non-methylated H3K4 by ADD_{3A}. Red dotted lines indicate hydrogen bonds (<3.3 Å) between H3 and ADD_{3A} residues. ADD_{3A} and H3 residues are represented as ball-and-stick models in green and yellow, respectively. (**A**) H3 peptide is shown with a F_o-F_c omit map contoured at 2.0 σ. (**B**) A close-up view of the recognition of the amino-terminus of the H3 tail by ADD_{3A}. (**C**) A close-up view of the Lys 4 binding pocket of ADD_{3A}. ADD_{3A}, ADD domain of DNMT3A.

Glu 578 of ADD_{3A} (Fig 3B; supplementary Fig S3 online). A 100-fold decreased affinity of the N-terminus acetylated H3 peptide to ADD_{3A} indicated the importance of N-terminus recognition (Table 1). The overall structure of the ADD_{3A}–H3 complex is similar to that of the ADD_{3L}–H3 complex, and the recognition mode of unmodified H3K4 is well conserved (Fig 3C; supplementary Figs S2A,B and S3 online). However, the affinity of ADD_{3A} for the H3 peptide is about 10-fold higher than that of ADD_{3L} (Table 1). The higher H3-binding affinity of ADD_{3A} might be attributable to the substitution of two residues, Ile 576 and Met 548, that are located at the histone interface of ADD_{3A}. A more detailed comparison is given in the supplementary information online.

In the ADD_{3A}–H3 tail structure, the side chain of H3R2 is fully exposed to solvent, as was previously observed in the DNMT3L–H3 complex structure (Ooi *et al*, 2007), implying that the methylation of H3R2 does not affect the affinity between H3 and ADD_{3A} (supplementary Fig S4 online). We examined the effect of asymmetrical dimethylation of H3R2, which is depleted from the active mammalian promoter and negatively correlated with H3K4me3 (Guccione *et al*, 2007), on the binding of H3 to ADD_{3A} using ITC. The $H3_{1-15}$ peptide carrying asymmetrically dimethylated H3R2 bound to ADD_{3A} with an affinity of 0.74 μM. This value is similar to the K_D value for the unmodified H3 peptide, indicating that the ADD_{3A}–H3 interaction is independent of the methylation status of H3R2.

The interaction surface of ADD_{3A} observed in the linked complex was consistent with that identified by NMR chemical-shift perturbation using the isolated H3 tail and ADD_{3A} (supplementary Fig S5 online), indicating that the interactions between ADD_{3A} and the H3 tail in the crystal are not artificially generated by the covalent link between them.

Fig 4 | Competitive binding of ADD_{3A} and $CD_{HP1\alpha}$ to the H3 tail. (**A**) GST pulldown assay analysed by SDS–PAGE and CBB staining. The GST–$CD_{HP1\alpha}$ bound to H3 K9me2 peptide in the absence of ADD_{3A} (lane 5) and was competed out by adding ADD_{3A} (lanes 6–9). (**B**) Reciprocal experiment of (**A**) using GST–ADD_{3A}, the H3 K9me3 peptide and $CD_{HP1\alpha}$. (**C**) ^1H–^{15}N HSQC spectra of the ^{15}N-labelled $CD_{HP1\alpha}$ in the ligand-free (green) and H3 K9me3-bound (red) forms are superimposed (left panel). The $CD_{HP1\alpha}$–H3 K9me3 complex was titrated with unlabelled ADD_{3A} (right panel). The cross-peak positions of ^{15}N-labelled $CD_{HP1\alpha}$ shifted from those of the H3-bound form to those of the free form during the titration. Selected spectral regions (i)–(iv) are magnified. (**D**,**E**) Reciprocally, ^{15}N-labelled ADD_{3A} in complex with H3K9me2 (**D**) or H3K9me3 peptide (**E**) was titrated by unlabelled $CD_{HP1\alpha}$. ADD, ATRX–DNMT3–DNMT3L; ADD_{3A}, ADD domain of DNMT3A; CBB, coomassie brilliant blue; $CD_{HP1\alpha}$, chromodomain of HP1α; GST, glutathione-*S*-transferase; HP1α, heterochromatin protein 1α; SDS–PAGE, sodium dodecyl sulphate–polyacrylamide gel electrophoresis.

Mutually exclusive H3 binding of DNMT3A and HP1

Several studies have showed that DNMTs are recruited to chromatin through interactions with chromo shadow domains (CSDs) of HP1 proteins (Fuks *et al*, 2003; Honda & Selker, 2008). The CD of HP1 proteins, which specifically binds to methylated H3K9, is indispensable for maintaining the condensed chromatin

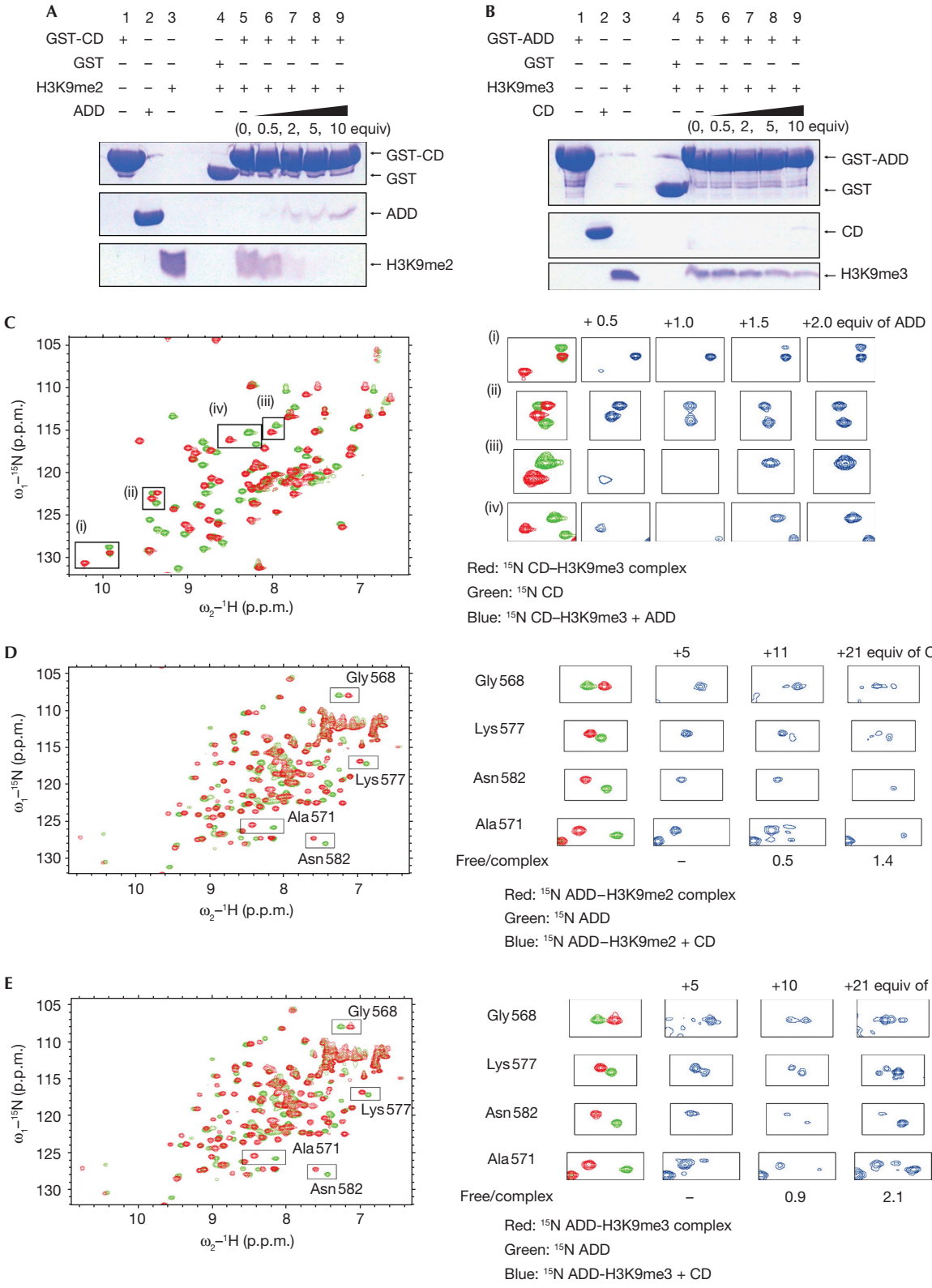

structure in heterochromatin regions. The model of the ternary complex of ADD_{3A}, $CD_{HP1\alpha}$ and H3 tail, which was built on the basis of the crystal structures of the ADD_{3A}–H3 and $CD_{HP1\alpha}$–H3 (Protein Data Bank entry; 3FDT) complexes (supplementary Fig S6 online), indicated that binding of $CD_{HP1\alpha}$ to the H3 tail might block ADD_{3A} binding, and vice versa, through steric occlusion of the H3 segment from Gln 5 to Thr 6. The H3 main chain from Ala1 to Thr 6 is covered with ADD_{3A}, whereas $CD_{HP1\alpha}$ binds to the main chain from Gln 5 to Arg 8.

We next examined whether ADD_{3A} and $CD_{HP1\alpha}$ bind simultaneously or exclusively to $H3_{1-19}$ containing H3K9me2 or H3K9me3 analogue using glutathione-*S*-transferase (GST) pull-down assays. The complexes of $CD_{HP1\alpha}$ and ADD_{3A} with K9me2/3 H3 tail were both observed (Fig 4A, lane 5, and Fig 4B, lane 5), but the ADD_{3A}–$CD_{HP1\alpha}$–H3 tail ternary complex was not seen (Fig 4A, lanes 6–9 and Fig 4B, lanes 6–9). A twofold molar excess of ADD_{3A} efficiently inhibited binding of K9me2 $H3_{1-19}$ to $CD_{HP1\alpha}$ (Fig 4A, lane 7). However, a 10-fold molar excess of $CD_{HP1\alpha}$ was needed to compete for roughly half of the peptide bound to ADD_{3A} (Fig 4B, lane 9). The mutually exclusive binding of $CD_{HP1\alpha}$ and ADD_{3A} to the H3 peptide was also shown by a competitive NMR titration experiment. The ^{1}H–^{15}N correlation spectrum of ^{15}N-labelled $CD_{HP1\alpha}$ in the presence of the non-labelled K9me3 H3 peptide showed a cross-peak pattern, indicating $CD_{HP1\alpha}$–H3 tail complex formation (Fig 4C, left panel). On titration of non-labelled ADD_{3A}, the cross-peak pattern shifted back to that of unliganded $CD_{HP1\alpha}$ in a slow exchange regime of an NMR timescale (Fig 4C, right panel). In the presence of twofold molar excess of ADD_{3A}, most of the cross-peaks of ^{15}N-labelled $CD_{HP1\alpha}$ are superimposable onto those of the free-form protein (supplementary Fig S7A online). The absence of direct interaction between ADD_{3A} and $CD_{HP1\alpha}$ was confirmed by adding unlabelled ADD_{3A} into ^{15}N-labelled $CD_{HP1\alpha}$ (supplementary Fig S7B online). Reciprocally, ^{1}H–^{15}N correlation experiments using ^{15}N-labelled ADD_{3A} showed that H3 binding of ADD_{3A} was perturbed by $CD_{HP1\alpha}$, albeit less efficiently. Additions of 21-fold and 10-fold molar excesses of $CD_{HP1\alpha}$ were required for dissociation of roughly 50% of the complexes of ADD_{3A} with the H3K9me2 and H3K9me3, respectively (Fig 4D,E). The K_D values of $CD_{HP1\alpha}$ for H3K9me3 and H3K9me2 were estimated to be $3.6 \pm 1.3\,\mu M$ and $7.0 \pm 3.2\,\mu M$, respectively, from the signal intensity ratio between the H3-bound and unliganded ^{15}N-labelled ADD_{3A} domains observed in the titration experiment. Although the interaction between ADD_{3A} and CSDs of HP1β has been previously observed in a GST pulldown assay (Fuks *et al*, 2003), the ADD_{3A}–H3 tail complex formation was not inhibited by the addition of $CSD_{HP1\alpha}$ in our NMR titration experiments and GST pulldown competition assays (data not shown).

DISCUSSION

Our structural and biochemical data clearly showed that the DNMT3A ADD domain specifically interacts with non-methylated H3K4, indicating a role of targeting DNMT activity to regions of chromatin lacking methylated H3K4. Conversely, it has previously been suggested that HP1 proteins promote DNA methylation in heterochromatic regions by interacting with both methylated H3K9 and DNMTs. Therefore, it is intriguing that ADD_{3A} and $CD_{HP1\alpha}$ are not able to bind simultaneously to the H3 tail: Our NMR and GST pulldown analyses indicate that ADD_{3A} can effectively dissociate $CD_{HP1\alpha}$ from the H3 tail, which is probably due to the higher H3 tail binding affinity of ADD_{3A} ($K_D = 0.25\,\mu M$) than that of $CD_{HP1\alpha}$ ($K_D = 1.3\,\mu M$; Table 1). DNMT enzymatic activity has been shown to be inhibited by nucleosomal structure and linker histones *in vitro*, despite the association of DNA methylation with repressive chromatin loci, indicating that temporal local loosening of condensed chromatin might be required for DNA methylation (Takeshima *et al*, 2008). The HP1 proteins are thought to be essential for maintenance of the heterochromatin structure (Schulze & Wallrath, 2007), as indicated by the observations that a point mutation within the H3 tail binding surface of CD of HP1 causes loosening of heterochromatin structure (Cryderman *et al*, 1998) and that tethering of HP1 to euchromatic regions leads to their heterochromatinization in *Drosophila* (Li *et al*, 2003). Recently, disruption of the interaction between the HP1β CD and K9me3 H3 tail has been shown to alter chromatin structure and facilitate H2AX phosphorylation in response to DNA damage (Ayoub *et al*, 2008). Thus, it is assumed that the dissociation of HP1 from the H3 tail might cause loosening of chromatin structures. HP1 proteins have been shown to be dynamically mobile and they are continuously exchanged in chromatin in the cells (Schmiedeberg *et al*, 2004). Therefore, once DNMT3A has been recruited to the chromatin complex, it is possible that ADD_{3A} competitively binds to H3 tails harbouring K9me2 or K9me3, displacing the HP1 proteins. Nevertheless, HP1 proteins that are released from the H3 tail might stay in the chromatin complex through interactions between their CSDs and chromatin-binding proteins (Eskeland *et al*, 2007). Together with the indication that relatively loose chromatin structure is required for DNMT enzymatic activity, it is tempting to speculate that H3 tail binding of ADD_{3A} might facilitate dissociation or rearrangement of HP1, which causes local loosening of heterochromatin structure at sites of *de novo* methylation. The affinity of ADD_{3A} to the K4me0 H3 tail is markedly higher than that of the ADD from DNMT3L ($K_D = 3.4\,\mu M$; Table 1), despite high sequence identity (54–55%). The affinity of the DNMT3L ADD domain for the H3 tail is comparable with those of CDs of HP1α, HP1β and HP1γ for the K9me3 H3 tail ($K_D = 13$, 3 and $7\,\mu M$, respectively; Fischle *et al*, 2005; Table 1 for $CD_{HP1\alpha}$). Thus, although the ADD domains of both DNMT3A and DNMT3L reside in the same DNMT3A–DNMT3L complex, they might have functionally distinct roles.

METHODS

Protein expression and purification. The human ADD_{3A} (residues 476–614) and the H3 tail (residues 1–20): ADD_{3A} fusion proteins were each bacterially expressed and purified using GST affinity and gel filtration column chromatography. The human HP1α CD ($CD_{HP1\alpha}$, residues 15–78) was bacterially expressed as a GST fusion. Detailed information about expression vectors and protein preparation is provided in the supplementary information online.

Histone H3 peptide preparation and *in vitro* binding assays. The H3 peptide was expressed in *Escherichia coli* as a GST-fusion protein and purified. Detailed information about GST-peptide purification and *in vitro* binding assays is available in the supplementary information online.

Structure determination. Crystals of ADD_{3A} were obtained in a hanging drop containing 2.0 μl protein solution mixed with 1.0 μl reservoir solution that contained 17% PEG 8000, 100 mM Tris–HCl, pH 8.5, and 200 mM $MgSO_4$. Crystals of H3-fused ADD_{3A}

were grown under the conditions of 10% PEG 2000 monomethyl ether and 100 mM Bis–Tris, pH 5.5. X-ray diffraction data sets were collected on the beamline BL-5A at the Photon Factory, Japan, at a temperature of 100 K in cryoprotectant solution containing 20% ethylene glycol. Data processing and structure determination are described in detail in the supplementary information online.

NMR spectroscopy. NMR spectra were recorded at 19 °C in 10 mM Tris–HCl, pH 7.0, 50 mM NaCl, 1 mM dithiothreitol, 10%(v/v) D_2O on a Bruker AVANCE 700. Spectra were processed using NMRpipe and analysed using Sparky (http://www.cgl.ucsf.edu/home/sparky). NMR spectra for ligand-free and H3-bound forms were made on the assumption of minimum chemical-shift perturbation. The same comparisons were also made for $CD_{HP1\alpha}$. Detailed information about NMR experiments is provided in the supplementary information online.

Coordinates. The structures of ADD_{3A} and the H3 tail–ADD_{3A} complex have been deposited in the Protein Data Bank (accession codes 3A1A and 3A1B).

Supplementary information is available at *EMBO reports* online (http://www.emboreports.org).

ACKNOWLEDGEMENTS

We thank N. Matsugaki, N. Igarashi, Y. Yamada, M. Suzuki and S. Wakatsuki for data collection at PF-BL-5; T. Nagase, U. Aapola and N. Tanese for cDNA of human DNMT3A, DNMT3L, and HP1α, respectively, and I. Hamachi and A. Ojida for support in ITC measurements. This work was supported by grants to M.S. from the Ministry of Education, Culture, Sports, Science and Technology (MEXT), Japan, and the Japan Science and Technology Agency, and also supported, in part, by the Global COE Program 'International Center for Integrated Research and Advanced Education in Materials Science', administered by the Japan Society for the Promotion of Science. This work was supported partly by the Grant-in-Aid for Scientific Research to S.I. from MEXT.

CONFLICT OF INTEREST

The authors declare that they have no conflict of interest.

REFERENCES

Argentaro A, Yang J, Chapman L, Kowalczyk M, Gibbons R, Higgs D, Neuhaus D, Rhodes D (2007) Structural consequences of disease-causing mutations in the ATRX–DNMT3–DNMT3L (ADD) domain of the chromatin-associated protein ATRX. *Proc Natl Acad Sci USA* **104:** 11939–11944

Ayoub N, Jeyasekharan A, Bernal J, Venkitaraman A (2008) HP1-beta mobilization promotes chromatin changes that initiate the DNA damage response. *Nature* **453:** 682–686

Bird A (2002) DNA methylation patterns and epigenetic memory. *Genes Dev* **16:** 6–21

Cryderman D, Cuaycong M, Elgin S, Wallrath L (1998) Characterization of sequences associated with position-effect variegation at pericentric sites in *Drosophila* heterochromatin. *Chromosoma* **107:** 277–285

El Gazzar M, Yoza B, Chen X, Hu J, Hawkins G, McCall C (2008) G9a and HP1 couple histone and DNA methylation to TNFalpha transcription silencing during endotoxin tolerance. *J Biol Chem* **283:** 32198–32208

Epsztejn-Litman S *et al* (2008) *De novo* DNA methylation promoted by G9a prevents reprogramming of embryonically silenced genes. *Nat Struct Mol Biol* **15:** 1176–1183

Eskeland R, Eberharter A, Imhof A (2007) HP1 binding to chromatin methylated at H3K9 is enhanced by auxiliary factors. *Mol Cell Biol* **27:** 453–465

Fischle W, Tseng B, Dormann H, Ueberheide B, Garcia B, Shabanowitz J, Hunt D, Funabiki H, Allis C (2005) Regulation of HP1-chromatin binding by histone H3 methylation and phosphorylation. *Nature* **438:** 1116–1122

Fuks F, Hurd P, Deplus R, Kouzarides T (2003) The DNA methyltransferases associate with HP1 and the SUV39H1 histone methyltransferase. *Nucleic Acids Res* **31:** 2305–2312

Goll M, Bestor T (2005) Eukaryotic cytosine methyltransferases. *Annu Rev Biochem* **74:** 481–514

Guccione E, Bassi C, Casadio F, Martinato F, Cesaroni M, Schuchlautz H, Lüscher B, Amati B (2007) Methylation of histone H3R2 by PRMT6 and H3K4 by an MLL complex are mutually exclusive. *Nature* **449:** 933–937

Honda S, Selker E (2008) Direct interaction between DNA methyltransferase DIM-2 and HP1 is required for DNA methylation in *Neurospora crassa*. *Mol Cell Biol* **28:** 6044–6055

Jackson J, Lindroth A, Cao X, Jacobsen S (2002) Control of CpNpG DNA methylation by the KRYPTONITE histone H3 methyltransferase. *Nature* **416:** 556–560

Lehnertz B, Ueda Y, Derijck A, Braunschweig U, Perez-Burgos L, Kubicek S, Chen T, Li E, Jenuwein T, Peters A (2003) Suv39h-mediated histone H3 lysine 9 methylation directs DNA methylation to major satellite repeats at pericentric heterochromatin. *Curr Biol* **13:** 1192–1200

Li Y, Danzer J, Alvarez P, Belmont A, Wallrath L (2003) Effects of tethering HP1 to euchromatic regions of the *Drosophila* genome. *Development* **130:** 1817–1824

Okitsu C, Hsieh C (2007) DNA methylation dictates histone H3K4 methylation. *Mol Cell Biol* **27:** 2746–2757

Ooi S *et al* (2007) DNMT3L connects unmethylated lysine 4 of histone H3 to *de novo* methylation of DNA. *Nature* **448:** 714–717

Schmiedeberg L, Weisshart K, Diekmann S, Meyer Zu Hoerste G, Hemmerich P (2004) High- and low-mobility populations of HP1 in heterochromatin of mammalian cells. *Mol Biol Cell* **15:** 2819–2833

Schulze S, Wallrath L (2007) Gene regulation by chromatin structure: paradigms established in *Drosophila melanogaster*. *Annu Rev Entomol* **52:** 171–192

Simon M, Chu F, Racki L, de la Cruz C, Burlingame A, Panning B, Narlikar G, Shokat K (2007) The site-specific installation of methyl-lysine analogs into recombinant histones. *Cell* **128:** 1003–1012

Tachibana M, Matsumura Y, Fukuda M, Kimura H, Shinkai Y (2008) G9a/GLP complexes independently mediate H3K9 and DNA methylation to silence transcription. *EMBO J* **27:** 2681–2690

Takeshima H, Suetake I, Tajima S (2008) Mouse Dnmt3a preferentially methylates linker DNA and is inhibited by histone H1. *J Mol Biol* **383:** 810–821

Weber M, Hellmann I, Stadler M, Ramos L, Pääbo S, Rebhan M, Schübeler D (2007) Distribution, silencing potential and evolutionary impact of promoter DNA methylation in the human genome. *Nat Genet* **39:** 457–466

Zhao Q *et al* (2009) PRMT5-mediated methylation of histone H4R3 recruits DNMT3A, coupling histone and DNA methylation in gene silencing. *Nat Struct Mol Biol* **16:** 304–311